Phosphorylation of the proline-rich domain of Xp95 modulates Xp95 interaction with partner proteins

Robert E. DeJOURNETT*†‡, Ryuji KOBAYASHI§, Shujuan PAN*†‡, Chuanfen WU‖, Laurence D. ETKIN‖, Richard B. CLARK¶, Oliver BÖGLER†‡ and Jian KUANG*[1]

*Department of Experimental Therapeutics, The University of Texas M.D. Anderson Cancer Center, 1515 Holcombe Blvd, Box 019, Houston, TX 77030, U.S.A., †Department of Neurosurgery and Neuro-Oncology, The University of Texas, M.D. Anderson Cancer Center, 1515 Holcombe Blvd, Box 019, Houston, TX 77030, U.S.A., ‡Program in Genes and Development, University of Texas Graduate School of Biomedical Sciences, Houston, TX 77030, U.S.A., §Department of Molecular Pathology, The University of Texas M.D. Anderson Cancer Center, 1515 Holcombe Blvd, Box 019, Houston, TX 77030, U.S.A., ‖Department of Molecular Genetics, The University of Texas M.D. Anderson Cancer Center, 1515 Holcombe Blvd, Box 019, Houston, TX 77030, U.S.A., and ¶Department of Integrative Biology and Pharmacology, The University of Texas Medical School, Houston, TX 77225, U.S.A.

The mammalian adaptor protein Alix [ALG-2 (apoptosis-linked-gene-2 product)-interacting protein X] belongs to a conserved family of proteins that have in common an N-terminal Bro1 domain and a C-terminal PRD (proline-rich domain), both of which mediate partner protein interactions. Following our previous finding that Xp95, the *Xenopus* orthologue of Alix, undergoes a phosphorylation-dependent gel mobility shift during progesterone-induced oocyte meiotic maturation, we explored potential regulation of Xp95/Alix by protein phosphorylation in hormone-induced cell cycle re-entry or M-phase induction. By MALDI–TOF (matrix-assisted laser-desorption ionization–time-of-flight) MS analyses and gel mobility-shift assays, Xp95 is phosphorylated at multiple sites within the N-terminal half of the PRD during *Xenopus* oocyte maturation, and a similar region in Alix is phosphorylated in mitotically arrested but not serum-stimulated mammalian cells. By tandem MS, Thr^{745} within this region, which localizes in a conserved binding site to the adaptor protein SETA [SH3 (Src homology 3) domain-containing, expressed in tumorigenic astrocytes] CIN85 (α-cyano-4-hydroxycinnamate)/SH3KBP1 (SH3-domain kinase-binding protein 1), is one of the phosphorylation sites in Xp95. Results from GST (glutathione S-transferase)-pull down and peptide binding/competition assays further demonstrate that the Thr^{745} phosphorylation inhibits Xp95 interaction with the second SH3 domain of SETA. However, immunoprecipitates of Xp95 from extracts of M-phase-arrested mature oocytes contained additional partner proteins as compared with immunoprecipitates from extracts of G_2-arrested immature oocytes. The deubiquitinase AMSH (associated molecule with the SH3 domain of signal transducing adaptor molecule) specifically interacts with phosphorylated Xp95 in M-phase cell lysates. These findings establish that Xp95/Alix is phosphorylated within the PRD during M-phase induction, and indicate that the phosphorylation may both positively and negatively modulate their interaction with partner proteins.

Key words: apoptosis-linked-gene-2 product (ALG-2)-interacting protein X (Alix), associated molecule with the Src homology 3 domain of signal transducing adaptor molecule (AMSH), M-phase phosphorylation, Src homology 3 domain-containing, expressed in tumorigenic astrocytes (SETA), *Xenopus* oocyte maturation, Xp95.

INTRODUCTION

Eukaryotic cells contain adaptor or scaffold proteins whose main functions are to bring proteins of related functions into proximity. Members of this class of proteins often contain multiple protein interaction sites, but lack enzymatic functions [1]. There is ample evidence that assembly of protein complexes by adaptor or scaffold proteins plays important roles in fundamental cellular processes such as cell cycle regulation and signal transduction [2–6]. During these processes, post-translational modifications, especially protein phosphorylation, often regulate interaction of adaptor/scaffold proteins with their binding partners [7,8]. Thus characterization of the phosphorylation of an adaptor/scaffold protein during a biological process may constitute an important step towards understanding regulation of its function.

The mammalian ALG-2 (apoptosis-linked-gene-2 product) interacting protein Alix (ALG-2-interacting protein X) belongs to a conserved family of proteins that have in common an N-terminal Bro1 domain (named after the yeast orthologue Bro1) and a C-terminal PRD (proline-rich domain) [9]. The Bro1 domain of the yeast orthologue, which consists of 387 amino acid residues, has been structurally defined [10–12]. The Alix Bro1 domain interacts with the endosomal sorting protein CHMP4b (charged multivesicular body protein 4b) and Src tyrosine kinase [10,11]. This domain also contains the highly conserved sequence motif KKDNDFIY at residues 312–319, which matches the Src autophosphorylation consensus sequence [12]. In this motif, Tyr^{319} is both a Src phosphorylation site and a docking site for the SH2 (Src homology 2) domain of Src [11]. The PRD contains multiple proline-rich motifs, which are potential binding sites for SH3-domain-containing proteins [5,13]. Previous studies have established that the N-terminal half of the Alix PRD interacts with the ubiquitin-ligase-like protein TSG101 (tumour susceptibility gene 101 product) at the residues 717–720 [14,15], the adaptor

Abbreviations used: ALG-2, apoptosis-linked-gene-2 product; Alix, ALG-2-interacting protein X; AMSH, associated molecule with the Src homology 3 domain of signal transducing adaptor molecule; CHMP4b, charged multivesicular body protein 4b; EGF, epidermal growth factor; EGFR, EGF receptor; ESCRT, endosomal sorting complexes required for transport; GST, glutathione S-transferase; HA, haemagglutinin; HEK-293 cell line, human embryonic kidney cell line; IOE, immature oocyte extract; LysC, lysyl endopeptidase; MALDI–TOF, matrix-assisted-laser desorption ionization–time-of-flight; MAPK, mitogen-activated protein kinase; MEE, M-phase egg extract; MOE, mature oocyte extract; MS/MS, tandem MS; PRD, proline-rich domain; SETA, Src homology 3 domain-containing, expressed in tumorigenic astrocytes; SH3, Src homology 3; STAM, signal transducing adaptor molecule; TSG101, tumour susceptibility gene 101 product; XSETA, *Xenopus* SETA.

[1] To whom correspondence should be addressed (email jkuang@mdanderson.org).

Table 1 PCR primers and vectors used in making cDNA construct

Amplified region	Template	PCR primers (forward/reverse)	Restriction sites	Cloning vector	Final product
Xp95 1–297	Xp95 cDNA	5′-CTCTGGATCCATGGCTACCTTCCTCGGTA-3′ 5′-GGACATCGATTCACATTACATATTCATC-3′	BamHI/ClaI	PCS2 + MT	P1–Myc
Xp95 298–602	Xp95 cDNA	5′-TAATGGATCCATGGACTTGGCTGACAAGATCAAC-3′ 5′-TCTGATCGATTTGTTACAGATATTGCCTC-3′	BamHI/ClaI	PCS2 + MT	P2–Myc
Xp95 603–867	Xp95 cDNA	5′-TGTAGGATCCATGCTGGATCAGATTTATGGAAGC-3′ 3′-GCATATCGATGTGGAGGGAAAAAAGGCTG-3′	BamHI/ClaI	PCS2 + MT	P3–Myc
Xp95 603–704	P3–Myc	5′-TGTAGGATCCATGCTGGATCAGATTTATGGAAGC-3′ 5′-ATATATCGATAGAATTCATCTCGCTCTGTTTT-3′	BamHI/ClaI	PCS2 + MT	P3A–Myc
Xp95 705–786	P3–Myc	5′-AGATGGATCCATGTTAAAGGATATACAACAAAGC-3′ 5′-AATCATCGATCTGCAGTTGGTGCTGGGTTAGA-3′	BamHI/ClaI	PCS2 + MT	P3B–Myc
Xp95 787–867	P3–Myc	5′-CCAAGGATCCATGGCTGCTGATTCTTCACAGCCT-3′ 3′-GCATATCGATGTGGAGGGAAAAAAGGCTG-3′	BamHI/ClaI	PCS2 + MT	P3C–Myc
Xp95 757–867	P3–Myc	5′-CCAAGGATCCATGGCTGCTGATTCTTCACAGCCT-3′ 3′GCATATCGATGTGGAGGGAAAAAAGGCTG-3′	BamHI/ClaI	PCS2 + MT	P3BC–Myc
XCIN85 1–374	IMAGE no. 4056834	5′-ATCGGAATTCTGATGGTGGAATACATTGTGGAATA-3′ 5′-ATCGTCTAGAATTACGTTGGAGTTAATTTCTTCTC-3′	EcoRI/XbaI	PCS2 + HA	XCIN85
Human Alix 603–869	Alix cDNA	5′-AGATGGATCCATGTTAAAGGATATACAACAAAGC-3′ 5′-AATCATCGATCTGCAGTTGGTGCTGGGTTAGA-3′	BamHI/ClaI	PCS2 + MT	Alix P3
Mouse Alix 1–868	Alix cDNA	5′-ATCGGGATCCATGGCGTCGTTCATCTGGGTG-3′ 5′-CGATCTCGAGTCTGCTGTGGATAGTAAGACTG-3′	BamHI/XhoI	pET30a	His–Alix

protein SETA (SH3-domain-containing expressed in tumorigenic astrocytes)/CIN85 (Cbl-interacting protein of 85 kDa)/SH3KBP1 (SH3-domain kinase-binding protein 1) at the residues 740–745 [13,16], endophilins at the residues 748–761 [17] and the Src protein tyrosine kinase at the residues 752–757 [11]. Previous studies on the role of Alix in the formation of multivesicular bodies and retroviral budding have demonstrated that Alix simultaneously binds TSG101 and CHMP4b, which are components of ESCRT (endosomal sorting complexes required for transport) I and III respectively and thus brings ESCRT I and ESCRT III complexes into proximity [14,15,18]. In EGFR [EGF (epidermal growth factor) receptor] endocytosis, Alix simultaneously binds SETA and endophilin, and formation of this complex has negative effects on EGFR endocytosis [19]. These findings establish the adaptor/scaffold role of Alix.

Despite the solid evidence that Alix plays adaptor/scaffold roles in diverse cellular processes, the regulation of Alix's function remains poorly understood due to lack of easily detectable post-translational modifications of Alix in any of the characterized biological processes that involve Alix's function. On the other hand, we previously demonstrated that Xp95, the *Xenopus* orthologue of Alix, undergoes a phosphorylation-dependent gel mobility shift during *Xenopus* oocyte maturation although the biological function of Xp95 was not characterized [12]. This established the first biological system that involves a prominent post-translational modification of a member in the Alix/Xp95 family of proteins. *Xenopus* oocyte maturation is a hormone-or growth-factor-induced process by which prophase-arrested *Xenopus* oocytes mature into M-phase-arrested fertilizable eggs through meiotic divisions [20,21]. This process consists of stimulus-induced signal transduction that leads to release of the prophase arrest and cell cycle re-entry and induction of various regulatory and structural events associated with M-phase induction [22]. Both of these processes are associated with elevated protein phosphorylation [5,23]. Since robust phosphorylation events during *Xenopus* oocyte maturation often represent conserved regulatory mechanisms in either of these processes [24], characterization of the Xp95 phosphorylation during *Xenopus* oocyte maturation and investigation of its conservation and functional implication may generate important insights on the regulation of this family of proteins. In the present study, we performed these studies and found that both Xp95 and Alix are phosphorylated within the N-terminal half of the PRD during M-phase induction. We also obtained evidence that these phosphorylations modulate their interaction with partner proteins.

MATERIALS AND METHODS

Plasmid construction, RNA production, oocyte injection and protein extraction

The pCS2 + MT-based RNA expression construct for Myc-epitope-tagged full-length Xp95 was described previously [25]. To create RNA expression constructs for Myc-epitope-tagged Xp95 fragments, encoding cDNA fragments were amplified from Xp95 cDNA by PCR. Xp95 mutants were created using the QuikChange® II site-directed mutagenesis kit (Stratagene, La Jolla, CA, U.S.A.), and primers were designed using PrimerX software (http://bioinformatics.org/primerx/) (Table 1). All plasmid DNAs were amplified in *Escherichia coli* and verified by DNA sequencing. The cDNA fragments were subcloned into pCS2 + MT vector. The plasmid DNA was linearized with NotI before being used for *in vitro* transcription using the mMESSAGE mMACHINE® kit (Ambion, Austin, TX, U.S.A.) according to the manufacturer's instructions. The RNA expression construct for HA (haemagglutinin)-tagged XSETA (*Xenopus* SETA) was created by PCR amplification of the encoding cDNA using a plasmid containing XSETA cDNA obtained from the IMAGE (Integrated Molecular Analysis of Genomes and their Expression) consortium (no. 4056834) as the template and subcloning of the cDNA into the pCS2 + HA vector.

Stage VI *Xenopus* oocytes were obtained, cultured and injected and proteins extracted as previously described [25]. *In vitro* dephosphorylation of proteins was performed by incubation of samples prepared in the absence of phosphatase inhibitors with five units of lambda phosphatase (New England Biolabs, Ipswich, MA, U.S.A.) at room temperature (23 °C) for 15 min.

Immunoblotting and immunoprecipitation

Immunoblotting and immunoprecipitation were performed according to our standard procedures [9,25]. Xp95 was immunoblotted with anti-Alix monoclonal antibodies [26]. GST (glutathione

S-transferase) or GST–Xp95-fusion proteins were immunoblotted with anti-GST polyclonal antibodies (Santa Cruz Biotechnology, Santa Cruz, CA, U.S.A.). Myc-epitope-tagged Xp95 products were immunoblotted with a monoclonal anti-(Myc epitope) antibody (Santa Cruz Biotechnology) and immunoprecipitated with polyclonal anti-(Myc epitope) antibodies (Santa Cruz Biotechnology). HA-epitope-tagged *Xenopus* SETA products were immunoblotted with a monoclonal anti-HA-epitope antibody (Roche Applied Sciences, Indianapolis, IN, U.S.A.) and immunoprecipitated with polyclonal anti-HA-epitope antibodies (Santa Cruz Biotechnology).

Determination of Xp95 phosphorylation sites by MS

Xp95 was partially purified from 15 ml of *Xenopus* oocyte or egg extracts as previously described [25]. The partially purified Xp95 samples were resolved by SDS/PAGE and stained with Coomassie Blue. Xp95 bands were excised and digested in-gel using 400 ng of *Achromobacter* protease I (LysC; Wako) for 22 h at 37 °C in 50 mM Tris/HCl (pH 9.0). The peptide fragments were extracted from the gel slice and concentrated using vacuum centrifugation. The digests were desalted using ZipTip C_{18} (Millipore) and eluted with 50 % acetonitrile containing 0.1 % TFA (trifluoroacetic acid). The samples were then analysed by MALDI–TOF (matrix-assisted laser-desorption ionization–time-of-flight) MS (Applied Biosystems 4700) using α-cyano-4-hydroxycinnamic acid. For MS/MS (tandem MS), the digests described above were further digested with 500 ng of thermolysin for 16 h at 37 °C in 30 mM ammonium bicarbonate buffer (pH 8.0) containing 2 mM calcium acetate, and products were desalted using ZipTip C_{18} and eluted with 50 % acetonitrile containing 1 % acetic acid. The samples were then analysed with a quadrupole TOF MS (Applied Biosystems MDS Sciex QSTAR) using nanospray with 1000 V [27].

Cell culture, transfection and synchronization

HeLa cells were cultured in McCoys 5A (Invitrogen, Carlsbad, CA, U.S.A.) that was supplemented with 2 mM L-glutamine and 10 % (v/v) fetal bovine serum (Atlanta Biologicals, Lawrenceville, GA, U.S.A.). HEK-293 cells were grown in DMEM (Dulbecco's modified Eagle's medium) with the same supplements. The mammalian expression vector for Myc-epitope-tagged Alix P3 was created by subcloning PCR-amplified cDNA that encodes Alix P3 into the pCS2 + MT vector. HeLa cells at 50 % confluence were transfected with 5 μg of the plasmid DNA using Lipofectamine™ 2000 (Invitrogen). To obtain mitotic cell lysates, HeLa cells were first treated with 2 mM thymidine (Invitrogen) for 12–15 h and then switched to fresh culture medium containing 0.1 μg/ml colcemid (Invitrogen). After 12–15 h, mitotic cells were selectively detached by gently tapping culture dishes 30 times. Detached cells were centrifuged at 1000 ***g*** for 5 min and lysed in 5 vol. of SDS/PAGE sample buffer.

Production of recombinant proteins

cDNA plasmids expressing GST-tagged Xp95 fragments in *E. coli* were produced using the PCR-based cloning procedure with primers and vectors summarized in Table 1. The bacterial expression vector for His-tagged Alix (His–Alix) was produced by cloning the open reading frame for mouse Alix into the pET30a vector via the PCR-based cloning procedure. cDNA plasmids expressing the GST-tagged second SH3 domain of human SETA and human endophilin B1b were obtained from Alexei Kurakin, Buck Institute for Age Research (Novato, CA, U.S.A.) [28] and Invitrogen respectively. The GST-tagged proteins were produced and purified as we previously described [12]. Production and purification of His–Alix were performed similarly except that bacteria lysates made in 20 mM sodium phosphate, 500 mM NaCl, 20 mM imidazole and 1 mM PMSF (pH 7.3) were absorbed with Ni Sepharose 6 Fast Flow resin (GE Healthcare) and eluted with 20 mM sodium phosphate, 500 mM NaCl and 500 mM imidazole (pH 7.3).

GST pull down and peptide binding/competition

IOE (immature oocyte extract) and MEE (M-phase egg extract) expressing HA–XSETA were incubated with 5 μg of either GST or GST–Xp95 fragments, for 4 h at 4 °C. The mixtures were then absorbed with glutathione-linked agarose beads (GE Healthcare) for 1 h, and the beads were washed extensively as described for immunoprecipitation. N-terminally biotinylated peptides consisting of the sequence TSSIPTPAPRTVFS or TSSIPpTPAPRTVFS were obtained from Chemicon (Temecula, CA, U.S.A.). Indicated amounts of these peptides dissolved in PBS were incubated with 1 μg of GST–SETA SH3 domain no. 2 in buffer MB (50 mM Hepes, 150 mM NaCl, 1 mM EDTA, 1 mM EGTA and 10 % glycerol) supplemented with freshly added 1 mM PMSF, 10 μg/ml aprotinin, 2 μg/ml leupeptin and 1 mM sodium vanadate and pulled down with strepavidin–Sepharose beads (GE Healthcare). Following three washes with buffer MB, bound proteins were eluted, separated by SDS/PAGE and stained with Coomassie Blue. These peptides were also incubated with 1 μg of SETA SH3 no. 2 GST and 10–25 ng of His–Alix and the mixtures were pulled down with glutathione–Sepharose beads. After three washes of the beads with buffer MB, bound proteins were eluted and separated by SDS/PAGE.

RESULTS

Xp95 is phosphorylated within the N-terminal half of the PRD during *Xenopus* oocyte maturation

In our initial efforts to characterize the Xp95 phosphorylation during *Xenopus* oocyte maturation, we characterized the region in Xp95 that is targeted by the phosphorylation. For this objective, one of our approaches was to analyse Xp95 purified from IOE or MEE by MALDI–TOF MS and identify a region that is specifically phosphorylated in the MEE Xp95. Xp95 was first partially purified from IOE or MEE by consecutive chromatography [25]. Immunoblotting of analytic quantities of partially purified Xp95 with cross-reactive anti-Alix monoclonal antibodies showed that the maturation-associated gel mobility shift of Xp95 was preserved (Figure 1A). Xp95 was then separated from other proteins by SDS/PAGE (Figure 1B) and digested in-gel with LysC (lysyl endopeptidase). Last, the LysC digests were analysed by MS to identify phosphorylated peptides. In principle, phosphopeptides identified by this method have a high probability of being physiologically relevant although some of phosphopeptides may not be identified for various reasons [29]. As shown in Figure 1(C), only one phosphopeptide was identified from the MEE Xp95, consisting of residues 706–756 and spanning the N-terminal half of the PRD. While this peptide from the IOE Xp95 had a single mass of 5080 Da (Figure 1D, left panel), which matches the theoretical mass of this peptide, this peptide from the MEE Xp95 showed three masses of 5080 Da, 5160 Da and 5240 Da (Figure 1D, right panel). Since each phosphorylation increases the mass by 80 Da in the MALDI–TOF MS, these results indicate that Xp95 is phosphorylated on at least two sites in this 5080 Da region during *Xenopus* oocyte maturation.

In the other approach, we made iterative subdivision of Xp95 into thirds (Figure 2A) and analysed each of the fragments that

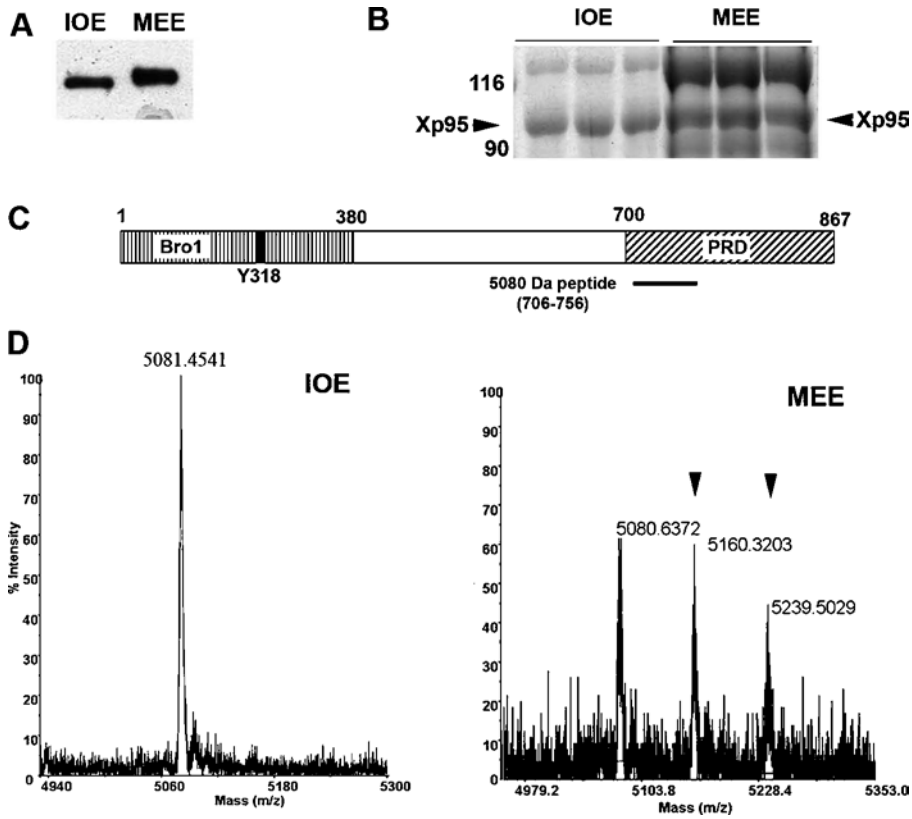

Figure 1 Identification of a phosphopeptide within the PRD by MS

(**A**) Partially purified Xp95 from IOE and MEE was immunoblotted with anti-Alix monoclonal antibodies. (**B**) Partially purified Xp95 from IOE or MEE was separated by SDS/PAGE and proteins were stained with Coomassie Blue. (**C**) A schematic illustration of the Bro1 domain and PRD in Xp95 and location of the 5080 Da peptide (residues 706–756). (**D**) Analysis of Xp95 peptides by MALDI–TOF MS. The 5080 Da fragment from IOE exists as a single non-modified form (left panel), whereas the 5080 Da fragment from MEE exists as non-modified, mono- and di-phosphorylated forms (right panel: phosphopeptides are indicated by arrowheads).

were N-terminally Myc-epitope-tagged and ectopically expressed in *Xenopus* oocytes for the ability to undergo a gel mobility shift in progesterone-matured *Xenopus* oocytes. An Xp95 fragment that is capable of undergoing a gel mobility shift during *Xenopus* oocyte maturation as the full-length Xp95 must contain a phosphorylation region although a fragment of Xp95 that contains all of the phosphorylation sites may not necessarily undergo a gel mobility shift if, for example, it lacks the kinase interaction site or certain structural information. As shown in Figure 2(B), the P1 (residues 1–297) or P2 (residues 298–602) fragment of Xp95 did not undergo a gel mobility shift in progesterone-matured oocytes. In contrast, the two products of the P3 fragment (residues 603–867), which might result from alternative translation start sites, both showed an easily detectable gel mobility shift in progesterone-matured oocytes, such that the upper band was partially shifted and the lower band was quantitatively shifted (Figure 2B, lanes 5 and 6). When the P3 fragment was further divided into thirds, only the P3B fragment (residues 705–786), which spans the N-terminal half of the PRD containing the 5080 Da region, showed the gel mobility shift in mature oocytes (Figure 2C). Further, phosphatase treatment of the P3B fragment from mature oocytes eliminated the gel mobility shift, confirming that the shift was due to phosphorylation (Figure 2D). These results concurred with the conclusion that Xp95 is phosphorylated in the 5080 Da region during *Xenopus* oocyte maturation and indicated that phosphorylation of this region is responsible for the maturation-associated gel mobility shift of Xp95. As further support to this conclusion, a P3B–P3C fusion product that was deleted from the 5080 Da region did not undergo the gel mobility shift (Figure 2E).

Since the 5080 Da region is only 30 residues shorter than P3B at the C-terminus, we wondered whether the 5080 Da region contains all of the structural information required for the shift-producing phosphorylation. To investigate this issue, we truncated P3B at the C-terminus by ten or 30 residues and examined the ability of the two products to undergo the maturation-associated gel mobility shift (Figure 2F). Neither of the truncation products recapitulated the gel mobility shift of the full-length P3B in mature oocytes, indicating that the last 30 residues of P3B contain structural information critical for phosphorylation of the 5080 Da region during *Xenopus* oocyte maturation.

Alix is phosphorylated in the N-terminal half of the PRD during M-phase induction

Xp95 and Alix are 65 % homologous in the N-terminal half of the PRD (Figure 3A), suggesting that Alix can also be phosphorylated by the kinase that phosphorylates Xp95 during *Xenopus* oocyte maturation. To test this possibility, we ectopically expressed a Myc-epitope-tagged P3-equivalent of Alix (Myc–Alix P3) in *Xenopus* oocytes by RNA injection and examined its gel mobility shift in progesterone-matured oocytes. As shown in Figure 3(B), Myc–Alix P3 underwent obvious gel mobility shifts in mature oocytes, supporting the conserved nature of the Xp95 phosphorylation during *Xenopus* oocyte maturation.

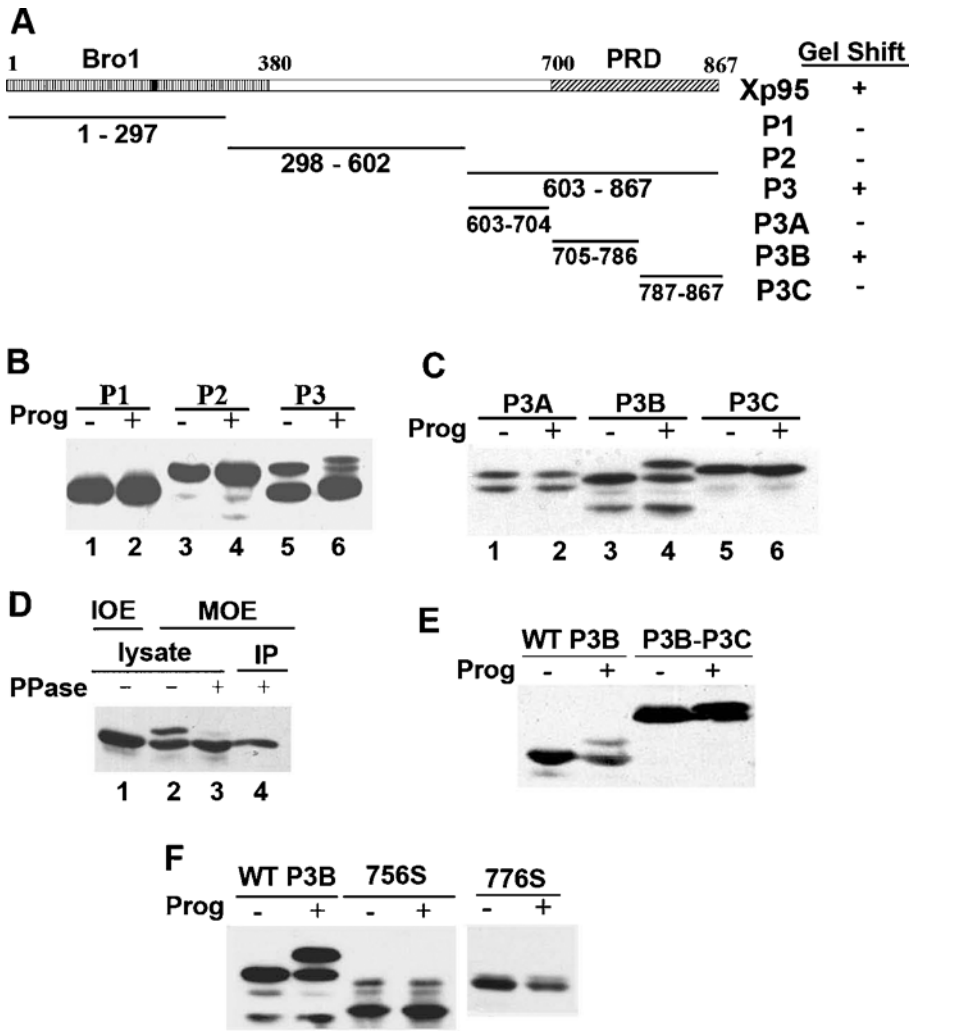

Figure 2 Phosphorylation of P3B within the PRD is responsible for the phosphorylation-dependent gel mobility shift of Xp95

(**A**) A schematic illustration of Xp95 fragments tested for the gel mobility shift in (**B**, **C**). (**B**, **C**) Indicated fragments of Xp95 that were Myc-epitope-tagged were expressed in *Xenopus* oocytes, and extracts of control or progesterone-matured oocytes were immunoblotted with an anti-Myc antibody. (**D**) Myc–P3B was expressed in *Xenopus* oocytes, and IOE and MOE were made of the injected oocytes. MOE or Myc–P3B immunoprecipitates were treated with lambda phosphatase, and products were immunoblotted with an anti-Myc antibody. (**E**) Myc-tagged P3B–P3C fusion was analysed as described above for the gel mobility shift. (**F**) Mutant Myc–P3B that was stopped at the residue 756 (756S) or the residue 776 (776S) was analysed as described above for the gel mobility shift.

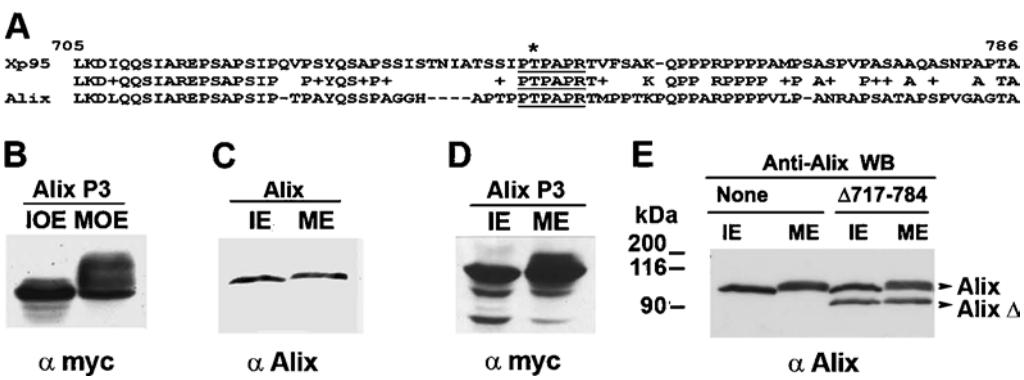

Figure 3 Alix is phosphorylated within the N-terminal half of the PRD during M-phase induction

(**A**) A sequence alignment of the P3B region of Xp95 with the equivalent region of Alix, in which the conserved SETA binding motif is underlined. (**B**) Myc–Alix P3 was expressed in *Xenopus* oocytes by RNA injection, and extracts of control (IOE) or progesterone-matured (MOE) oocytes were immunoblotted with an anti-Myc antibody. (**C**) Protein lysates of randomly growing (IE) and mitotically arrested (ME) HeLa cells were immunoblotted with anti-Alix antibodies. (**D**) Protein lysates of randomly growing (IE) and mitotically arrested (ME) HeLa cells that ectopically expressed Myc–Alix P3 were immunoblotted with anti-Myc antibodies. (**E**) Protein lysates of randomly growing (IE) and mitotically arrested (ME) HeLa cells that were mock treated or ectopically expressed AlixΔ717–784 were immunoblotted with anti-Alix antibodies.

Xenopus oocyte maturation consists of mitogen-induced cell cycle entry and M-phase induction. As initial steps to determine which of these processes involves the Xp95/Alix phosphorylation and to determine if Alix is phosphorylated under similar circumstances in mammalian cells, we examined the gel mobility shift of Alix in HeLa cells that were arrested at metaphase by the microtubule poison colcemid and in NIH 3T3 cells during serum stimulation of cell cycle re-entry. No gel mobility shift was detected in Alix during the cell cycle re-entry of NIH 3T3 cells by immunoblotting of crude cell lysates with anti-Alix antibodies (results not shown). In contrast, a quantitative gel mobility shift was detected by the same method in Alix from metaphase-arrested HeLa cells (Figure 3C). Next, we ectopically expressed Myc–Alix P3 in HeLa cells by cDNA transfection and immunoblotted crude lysates made of randomly growing or mitotically arrested cells with an anti-Myc antibody. Gel mobility shifts were observed in Myc–AlixP3 from M-phase-arrested HeLa cells (Figure 3D). Further, we ectopically expressed a FLAG-tagged Alix with an internal deletion at residues 717–784 (FLAG–AlixΔ717–784), a region very similar to the P3B region in Xp95, and examined its gel mobility shift in metaphase-arrested HeLa cells by immunoblotting of crude cell lysates. No gel mobility shift was observed in FLAG–AlixΔ717–784, while an obvious gel mobility shift was observed in the endogenous full-length Alix on the same immunoblot (Figure 3E). Together, these results indicated that Alix is phosphorylated in the N-terminal half of the PRD during M-phase induction and implied that the maturation-associated phosphorylation of Xp95 is an event that associates with M-phase induction.

One of the phosphorylation sites in the 5080 Da region of Xp95 is Thr^{745}

The 5080 Da region contains 16 potential phosphorylation sites out of the total 50 amino acid residues as well as docking sites for multiple SH3-domain-containing proteins. Thus, to explore the functional implication of the Xp95/Alix phosphorylation during M-phase induction, we characterized the amino acid residues in the 5080 Da region that are phosphorylated during *Xenopus* oocyte maturation by MS/MS. For this, the LysC-digested Xp95 from MEE was further digested with thermolysin, and resultant smaller peptides were sequenced by MS/MS, in which one phosphorylation increases mass by 40 Da. Results from multiple attempts consistently showed that Thr^{745} in the sequence context SSIPTPAPRT was phosphorylated (Figures 4A and 4B) although the other phosphorylation site in the 5080 Da region could not be identified. Sequence alignment of the peptide with the Alix equivalent showed that PTPAPR contained in this sequence matches the binding sites for SETA (Figure 3A), indicating that Xp95 is phosphorylated in the SETA binding site during *Xenopus* oocyte maturation.

In our attempt to identify the other phosphorylation site, we performed site-directed mutagenesis of all of the potential phosphorylation sites in the 5080 Da region (schematically diagrammed in Figure 5A) and examined the effect on the gel mobility shift of P3B in mature oocytes. The T745A mutation did not eliminate the gel mobility shift (Figure 5B), and neither did other point mutations. We then made various double or triple mutations of the potential phosphorylation sites or small deletions as summarized in Figure 5(C) and examined the effect on the gel mobility shift of P3B. None of the mutations eliminated the gel mobility shift of P3B (Figure 5D), raising the possibility that the shift-producing phosphorylation of the 5080 Da region occurs at non-restricted sites.

The Thr^{745} phosphorylation negatively regulates Xp95 interaction with SETA

To explore the functional implication of M-phase-associated phosphorylation of Xp95/Alix, we initially determined the effect of the Thr^{745} phosphorylation on Xp95 interaction with SETA. For this objective, we produced recombinant protein encoding the second SH3 domain of rat SETA fused with GST (GST–SETA SH3) in bacteria and examined its interaction with Xp95 in IOE and MOE by GST-pull down assays. The second SH3 domain of SETA was selected because it most efficiently interacts with Alix [3]. As shown in Figure 6(A), GST–SETA SH3 pulled down 10-fold more Xp95 from IOE than from MOE, indicating that the Thr^{745} phosphorylation of Xp95 inhibits Xp95 interaction with SETA. To test this hypothesis, we first expressed an HA-tagged *Xenopus* orthologue of human SETA (HA–XSETA), which contains equivalents of the three SH3 domains of human SETA, in *Xenopus* oocytes by RNA injection, and induced oocyte maturation with progesterone in half of them. We then incubated bacterially produced GST–Xp95P3, which is presumably not phosphorylated, with extracts made of these oocytes and examined its interaction with HA–XSETA in IOE and MOE. In contrast with the preferential interaction of GST–SETA SH3 with Xp95 in IOE, GST–Xp95P3 pulled down similar levels of HA–XSETA from IOE and MOE (Figure 6B). These data eliminated the possibility that the decreased interaction of GST–SETA SH3 with Xp95 in MOE is due to a modification of the SETA protein. Secondly, we obtained biotinylated Thr^{745} non-phosphorylated and phosphorylated peptides of Xp95 that contain the entire SETA binding site and tested their interaction with GST–SETA SH3 by peptide binding and competition assays. In the peptide binding assay, increasing concentrations of these two peptides, bound to streptavidin beads, were incubated with GST–SETA SH3, and relative concentrations of the two peptides required for binding to GST–SETA SH3 were determined. The phosphorylated peptide recovered a similar level of GST–SETA SH3 at a 10-fold higher concentration as compared with the unphosphorylated peptide (Figure 6C). In the peptide competition assay, we incubated recombinant His-tagged Alix (His–Alix) with GST–SETA SH3 in the presence of increasing concentrations of either peptide (Figure 6D). While 1 μg of the unphosphorylated peptide completely inhibited interaction of GST–SETA SH3 with His–Alix, this amount of the phosphorylated peptide did not eliminate the interaction (Figure 6D). In a control assay, neither of the peptides interfered with the interaction between Alix and endophilin (Figure 6E), which is mediated by an SH3 domain in endophilin but a different proline-rich motif in Alix. These results support the hypothesis that the Thr^{745} phosphorylation negatively regulates Xp95 interaction with SETA.

Phosphorylation of the N-terminal half of the PRD may also positively regulate Xp95 interaction with partner proteins

To further explore the functional implication of M-phase-associated phosphorylation of Xp95/Alix at the N-terminal half of the PRD, we expressed Myc-epitope-tagged Xp95 (Myc–Xp95) in *Xenopus* oocytes by RNA injection and immunoprecipitated the protein from extracts of control or progesterone-matured oocytes with anti-Myc antibodies. Coomassie Blue staining of SDS/PAGE-separated proteins revealed that the Myc–Xp95 immunocomplex from immature oocytes contained Myc–Xp95, heavy and light chains of IgG and a low-molecular-mass protein of unknown identity. Besides these proteins, the Myc–Xp95 immunocomplex from mature oocytes contained several additional proteins, which sized between the IgG heavy chain and the 90 kDa

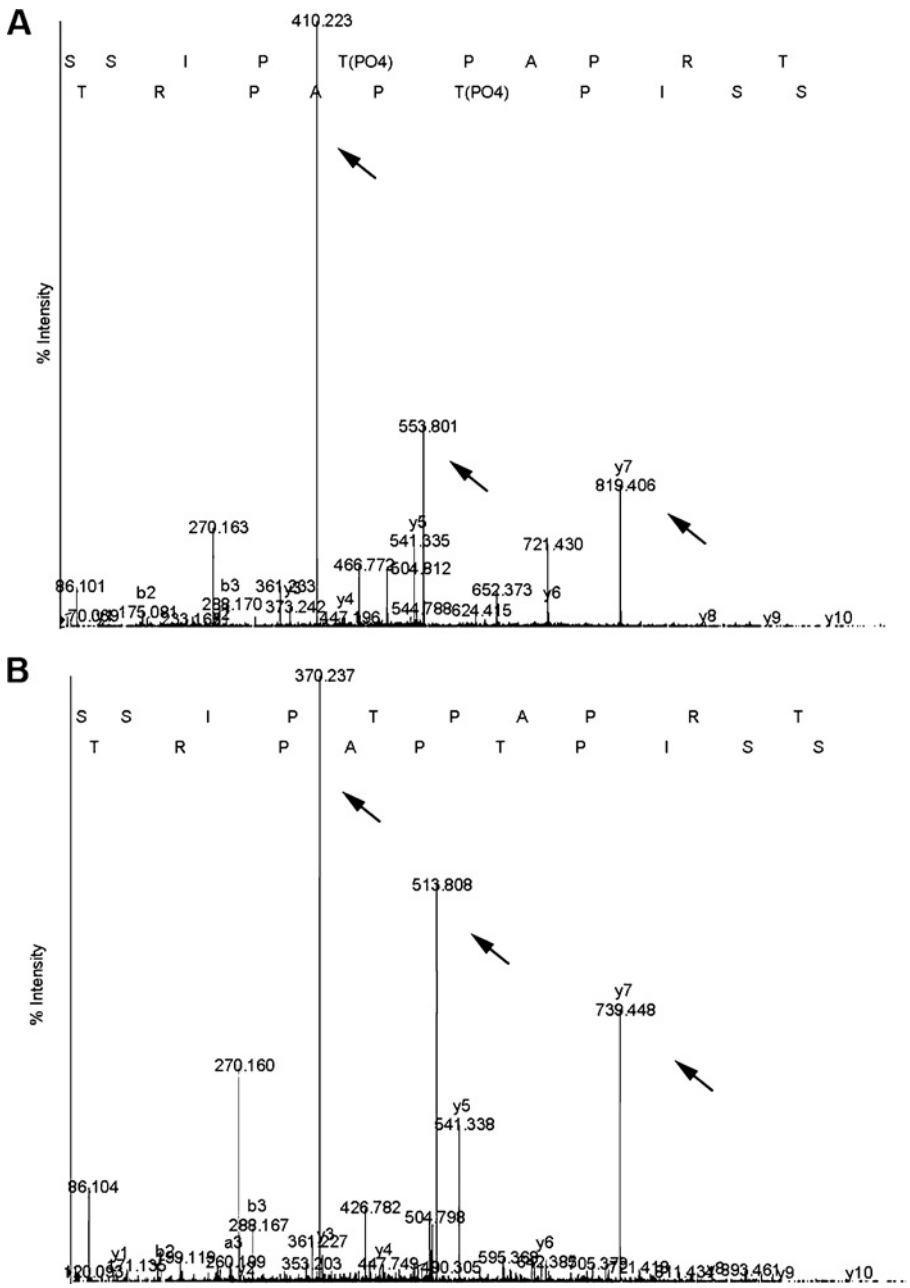

Figure 4 Identification of Thr[745] as a phosphorylation site in the 5080 Da region

Tandem mass spectra of phosphorylated (**A**) and unphosphorylated (**B**) peptides showing Thr[745] phosphorylation. y5 ion presents as 541.33 in both MEE (panel A) and IOE (panel B), whereas y6 and y7 ions in MEE are 80 mass units larger than those in IOE. The doubly charged ions of the peptides (513.8 for IOE and 553.8 for MEE) and y7 ions (370.237 in IOE and 410.223 in MEE) show 40 mass unit differences between IOE and MEE (arrows indicate ions).

molecular mass marker (Figure 7A) and were not recognized by the anti-Myc antibodies (results not shown). These results indicated that M-phase-associated phosphorylation of Xp95 may positively regulate Xp95 interaction with partner proteins. Although testing this hypothesis, which requires determination of the identity of the additional proteins in the Myc–Xp95 immunocomplex from mature oocytes, mapping each of their interaction sites in Xp95 and comparing each of their interactions with Xp95 from immature and mature oocytes, is beyond the scope of the present study, this hypothesis inspired us to examine the impact of Xp95 phosphorylation on the deubiquitinase AMSH (associated molecule with the SH3 domain of signal transducing adaptor molecule). AMSH has been functionally linked to the endosomal sorting machinery like Alix [30–34]; however, no physical connection, either direct or indirect, had been detected between AMSH and Alix [30,31]. We ectopically expressed Myc–Xp95 in HEK-293 cells (human embryonic kidney cells) that were either growing randomly or mitotically arrested and determined the interaction of Myc–Xp95 with GST-tagged AMSH (GST–AMSH) or GST–SETA SH3 (used as a control). While GST–SETA SH3 specifically interacted with GFP-Xp95 in interphase cell lysates as expected, the converse was observed with GST–AMSH, as GST–AMSH specifically interacted with Myc–Xp95 in mitotic cell lysates (Figure 7B). Further, His–Alix did not interact with

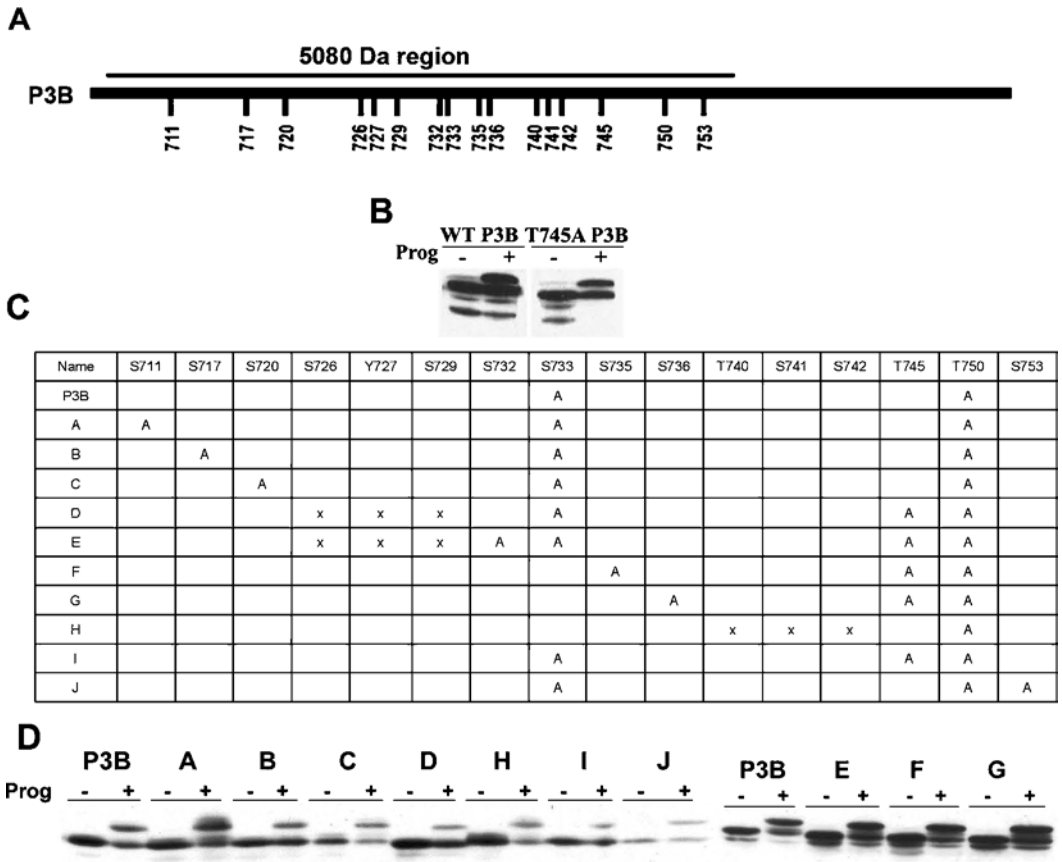

Name	S711	S717	S720	S726	Y727	S729	S732	S733	S735	S736	T740	S741	S742	T745	T750	S753
P3B								A							A	
A	A							A							A	
B		A						A							A	
C			A					A							A	
D				x	x	x		A						A	A	
E				x	x	x	A	A						A	A	
F									A					A	A	
G										A				A	A	
H											x	x	x		A	
I								A						A	A	
J								A							A	A

Figure 5 None of the potential phosphorylation sites in the 5080 Da region is required for the gel mobility shift of P3B

(**A**) A schematic illustration of the residues that were individually mutated in the 5080 Da region of Myc–P3B. (**B**) Wild-type Myc–P3B (WT P3B) and the T745A mutant form of Myc–P3B (T745A P3B) were assayed in parallel for the gel mobility shift as described in Figure 2. (**C**) A summary of multiple-site mutations made in the 5080 Da region of Myc–P3B. 'A' represents a point mutation to alanine, and 'X' represents a deletion mutation. (**D**) Indicated Myc–P3B mutants were assayed for the gel mobility shift during oocyte maturation as described in Figure 2.

GST–AMSH *in vitro*, suggesting that a post-translational modification is required for AMSH–Alix interaction (results not shown). These results support the hypothesis that M-phase-associated phosphorylation of the PRD is capable of positively modulating Xp95/Alix interaction with a group of partner proteins.

DISCUSSION

The phosphorylation of Xp95, which underlies its gel mobility shift during *Xenopus* oocyte maturation, is likely to be a regulatory event of Xp95's function. Therefore elucidation of the regions/residues involved should provide important information on Xp95 regulation. As Xp95 is 87 % homologous with mammalian Alix, we furthermore expected that post-translational modifications that regulate Xp95 are conserved in Alix. However, as biochemical analyses are easier in the *Xenopus* system, where large amounts of proteins can be easily generated, we pursued our discoveries there and sought confirmation of our findings in mammalian cells.

By the direct approach of MS, we discovered one region in Xp95 that is phosphorylated on at least two sites during *Xenopus* oocyte maturation, and identified Thr^{745}, which is within the SETA binding motif [13,16], as one of the phosphorylation sites. We further demonstrated by Xp95–SETA interaction and peptide binding/competition assays that the Thr^{745} phosphorylation is an M-phase-associated event that inhibits Xp95 binding to the second SH3 domain of SETA. These findings indicate that phosphorylation of Xp95/Alix at the SETA binding site inhibits Xp95/SETA interaction and suggest that the cellular process that involves this interaction is down-regulated during M-phase induction. We should note that since Thr^{745} of Xp95 lies in an S/T-P motif, we tested whether CDC2 (cell division cycle 2 kinase)/cyclin B or p42 MAPK (mitogen-activated protein kinase), the two major proline-directed protein kinases in mature *Xenopus* oocytes, could phosphorylate Xp95 *in vitro*. Negative results were obtained from multiple attempts with either of the kinases (results not shown), suggesting that Xp95 is targeted by a different mitotic kinase.

Since MS-based analysis of protein phosphorylation is often low-yield, we additionally mapped the region and sites in Xp95 whose phosphorylation is responsible for the gel mobility shift of Xp95 during *Xenopus* oocyte maturation. By iterative subdivision of Xp95 into thirds and testing various fragments for the gel mobility shift, we found that the P3B fragment (residues 706–786), which spans the N-terminal half of the PRD, retains the ability to undergo the phosphorylation-dependent gel mobility shift during *Xenopus* oocyte maturation. This finding is consistent with the MS data, as the P3B fragment not only contains the entire 5080 Da region (residues 706–756) but, as shown by further mapping data, also requires its presence for the gel mobility shift of P3B.

The 5080 Da region contains 16 potential phosphorylation sites out of the total 50 amino acid residues, representing a great enrichment of phosphorylatable residues: 32 % as compared with 18 %

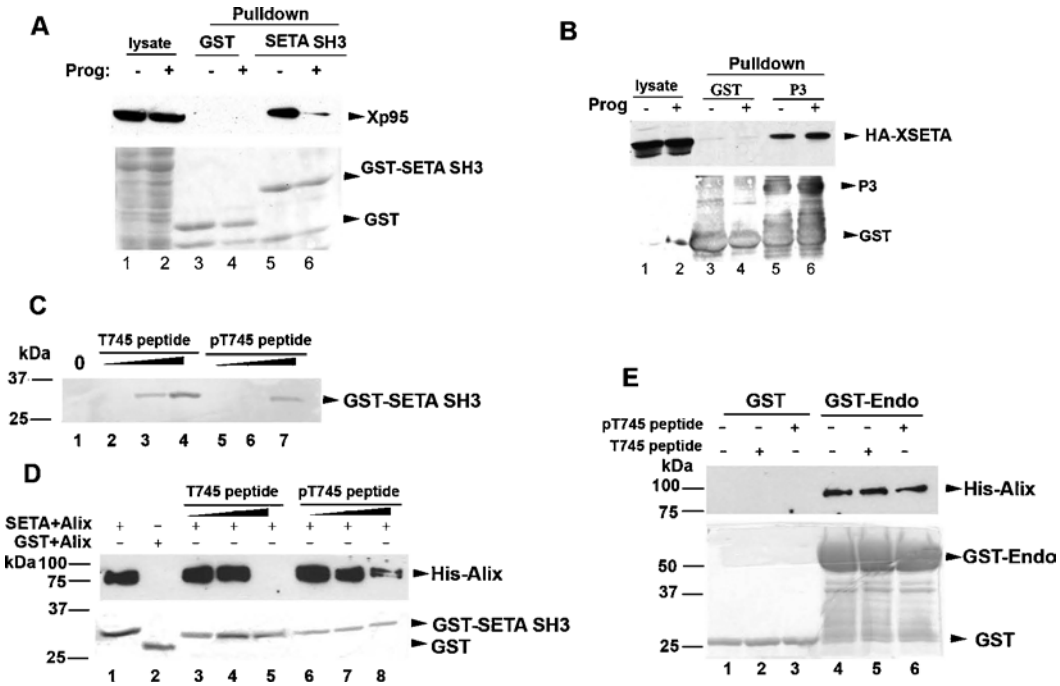

Figure 6 Xp95 phosphorylation at Thr^{745} inhibits SETA binding

(**A**) After GST or GST-tagged second SH3 domain of SETA (SETA SH3) was incubated with extracts of control or progesterone-matured oocytes, crude lysates or proteins pulled down by glutathione–Sepharose beads were immunoblotted with anti-Alix antibodies (upper panel) or stained with Coomassie Blue (lower panel). (**B**) After GST or GST-tagged P3 fragment of Xp95 was incubated with extracts of control or progesterone-matured oocytes that ectopically expressed HA-tagged *Xenopus* SETA (HA–XSETA), crude cell lysates or proteins pulled down by glutathione–Sepharose beads were immunoblotted with anti-HA antibodies (upper panel) or stained with Coomassie Blue (lower panel). (**C**) Increasing amounts (10, 100 and 1000 ng) of the Thr^{745} non-phosphorylated (T745 peptide) or phosphorylated (pT745 peptide) peptide immobilized on to strepavidin beads were incubated with GST–SETA SH3, and bound proteins were immunoblotted with anti-GST antibodies. (**D**) GST–SETA SH3 was incubated with His-tagged Alix in the presence of increasing amounts (10, 100 and 1000 ng) of T745 peptide (lanes 3–5) or pT745 peptide (lanes 6–8), and proteins pulled down by glutathione–Sepharose beads were immunoblotted with anti-Alix antibodies (upper panel) or stained with Coomassie Blue (lower panel). (**E**) GST or GST-tagged endophilin (GST–Endo) was analysed as described in (**D**).

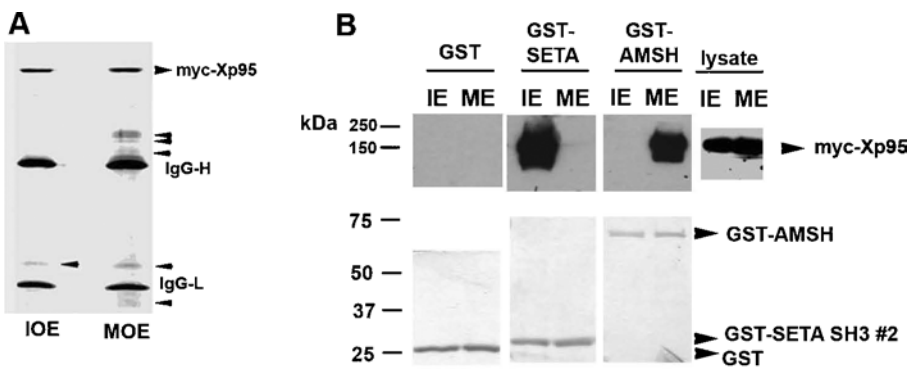

Figure 7 Phosphorylation of Xp95 correlates with its interaction with additional partner proteins

(**A**) Ectopically expressed Xp95 was immunoprecipitated from extracts of immature (IOE) or mature (MOE) oocytes, and the immunocomplexes were analysed by SDS/PAGE and Coomassie Blue staining. (**B**) GST, GST–SETA SH3 or GST–AMSH was incubated with crude lysates of randomly growing (IE) or mitotically arrested (ME) HEK-293 cells, and proteins pulled down by glutathione–Sepharose were immunoblotted with an anti-Myc antibody (upper panel) or stained with Coomassie Blue (lower panel).

in the protein overall. Since MS revealed only one of the phosphorylation sites, we tried to identify the second phosphorylation site in the 5080 Da region by mutagenesis and gel mobility shift assays. Mutation of Thr^{745} to alanine did not eliminate the gel mobility shift of P3B, supporting the existence of a second site. However, mutation of any one of the other potential phosphorylation sites in this region also failed to eliminate the shift, suggesting that phosphorylation in the 5080 Da region can occur at varied sites among which Thr^{745} is phosphorylated more often. The potentially non-strict nature of the P3B phosphorylation also makes it possible that phosphorylation of the 5080 Da region in Xp95 during *Xenopus* oocyte maturation is a heterogeneous event, with individual proteins showing different modifications. This may account for the lack of success in identifying the second phosphorylation site by the MS/MS.

One plausible explanation for the region-specific but site-flexible phosphorylation of Xp95 during M-phase induction is that the responsible kinase forms a stable complex with Xp95. In principle, the specificity of a protein kinase towards a substrate depends on the substrate concentration. When a kinase forms a

stable complex with its substrate, the bound substrate is at an infinitely high concentration and thus accessible domains may be phosphorylated non-specifically. This phenomenon has been described in phosphorylation of the yeast Swe1 by mitotic CDK (cyclin-dependent kinase) complex [35]. Under this hypothesis, the results showing that the 5080 Da region alone did not recapitulate the shift of P3B suggest the possibility that the portion of P3B outside the 5080 Da region contains structural information required for kinase interaction. From a functional point of view, the non-strict nature of the phosphorylation of the 5080 Da region may imply that phosphorylation functions to increase the negative charge in this region rather than only affecting specific docking sites for partner proteins. In principle, the increased negative charge in the 5080 Da region may potentially modulate the conformation of Xp95, its dimerization, or its intramolecular interaction, which in turn affects Xp95 interaction with partner proteins. These possibilities will be explored in future studies. By comparing the prominent components in Xp95 immunoprecipitates, we observed additional partner proteins in the Xp95 complex from mature oocytes as compared with immature oocytes. We also found an example of a specific protein, AMSH, which preferentially binds to phosphorylated Xp95 in M-phase cell lysates. Although we have not yet resolved whether the interaction between Xp95 and AMSH is direct or indirect (since bacterial protein used for *in vitro* binding assays are presumably not phosphorylated), these results strengthen the hypothesis that site-flexible phosphorylation of the 5080 Da region promotes Xp95 interaction with a group of partner proteins.

Xenopus oocyte maturation consists of both progesterone-induced signal transduction and meiotic inductions [22], and we previously suggested that the Xp95 gel mobility shift associates with progesterone-induced signal transduction based on the correlation of the Xp95 phosphorylation with activation of p42 MAPK [25]. However, these two processes overlap during progesterone-induced *Xenopus* oocyte maturation, making it difficult to unambiguously address this issue using this experimental system. By observing the Alix gel mobility shift during growth factor-induced cell cycle re-entry and mitotic arrest of cultured somatic cells, we resolved that the phosphorylation-dependent gel mobility shift of Alix/Xp95 is an M-phase-associated event. Alix has been demonstrated to be involved in multiple stages of endosome trafficking, including endocytosis of activated growth factor receptors and formation of multivesicular late endosomes [14,19,36,37]. Alix has also been shown to bind focal adhesion kinases and regulate cell adhesion [26,38]. Our recent studies have demonstrated that Alix is an F-actin-binding protein in mammalian fibroblast cells that promotes actin-cytoskeleton assembly [26]. Since M-phase induction involves disassembly of cytoplasmic membrane trafficking systems, reorganization of the actin cytoskeleton and inhibition of cell adhesion [39–41], the association of Xp95/Alix phosphorylation with M-phase raises the possibility that this modification of Xp95/Alix modulates its roles in these cellular processes during M-phase induction.

This work was supported by American Cancer Society grant RPG-00-071-01-DDC and NIH (National Institutes of Health)/NCI (National Cancer Institute) grant 1 RO1 CA93941 awarded to J. K. and 1R01CA108500 awarded to O. B. The MS work was performed in The Proteomics Core Facility at The University of Texas M. D. Anderson Cancer Center. DNA sequencing was performed by the DNA Analysis Facility of UT M. D. Anderson Cancer Center, which is supported by NCI grant CA-16672. We thank Dr A. Kurakin for kindly providing the plasmid for expressing the GST-tagged second SH3 domain of human SETA and Ms J. Friedman for editorial assistance.

REFERENCES

1 Dikic, I. (2002) CIN85/CMS family of adaptor molecules. FEBS Lett. **529**, 110–115
2 Schmitt, A. and Nebreda, A. R. (2002) Signalling pathways in oocyte meiotic maturation. J. Cell Sci. **115**, 2457–2459
3 Borinstein, S. C., Hyatt, M. A., Sykes, V. W., Straub, R. E., Lipkowitz, S., Boulter, J. and Bogler, O. (2000) SETA is a multifunctional adapter protein with three SH3 domains that binds Grb2, Cbl, and the novel SB1 proteins. Cell. Signalling **12**, 769–779
4 Zell, T., Warden, C. S., Chan, A. S., Cook, M. E., Dell, C. L., Hunt, III, S. W. and Shimizu, Y. (1998) Regulation of β1-integrin-mediated cell adhesion by the Cbl adaptor protein. Curr. Biol. **8**, 814–822
5 Birge, R. B., Knudsen, B. S., Besser, D. and Hanafusa, H. (1996) SH2 and SH3-containing adaptor proteins: redundant or independent mediators of intracellular signal transduction. Genes Cells **1**, 595–613
6 Scaife, R. M., Courtneidge, S. A. and Langdon, W. Y. (2003) The multi-adaptor proto-oncoprotein Cbl is a key regulator of Rac and actin assembly. J. Cell Sci. **116**, 463–473
7 Gaston, I., Johnson, K. J., Oda, T., Bhat, A., Reis, M., Langdon, W., Shen, L., Deininger, M. W. and Druker, B. J. (2004) Coexistence of phosphotyrosine-dependent and -independent interactions between Cbl and Bcr-Abl. Exp. Hematol. **32**, 113–121
8 Liu, J., Kimura, A., Baumann, C. A. and Saltiel, A. R. (2002) APS facilitates c-Cbl tyrosine phosphorylation and GLUT4 translocation in response to insulin in 3T3-L1 adipocytes. Mol. Cell. Biol. **22**, 3599–3609
9 Wu, Y., Pan, S., Che, S., He, G., Nelman-Gonzalez, M., Weil, M. M. and Kuang, J. (2001) Overexpression of Hp95 induces G_1 phase arrest in confluent HeLa cells. Differentiation **67**, 139–153
10 Kim, J., Sitaraman, S., Hierro, A., Beach, B. M., Odorizzi, G. and Hurley, J. H. (2005) Structural basis for endosomal targeting by the Bro1 domain. Dev. Cell **8**, 937–947
11 Schmidt, M. H., Dikic, I. and Bogler, O. (2005) Src phosphorylation of Alix/AIP1 modulates its interaction with binding partners and antagonizes its activities. J. Biol. Chem. **280**, 3414–3425
12 Geahlen, R. L. and Harrison, M. L. (1990) Protein-tyrosine kinases. In Peptides and Protein Phosphorylation (Kemp, B. E., ed.), pp. 239–253, CRC Press, Boca Raton
13 Kowanetz, K., Szymkiewicz, I., Haglund, K., Kowanetz, M., Husnjak, K., Taylor, J. D., Soubeyran, P., Engstrom, U., Ladbury, J. E. and Dikic, I. (2003) Identification of a novel proline-arginine motif involved in CIN85-dependent clustering of Cbl and down-regulation of epidermal growth factor receptors. J. Biol. Chem. **278**, 39735–39746
14 Strack, B., Calistri, A., Craig, S., Popova, E. and Gottlinger, H. G. (2003) AIP1/ALIX is a binding partner for HIV-1 p6 and EIAV p9 functioning in virus budding. Cell **114**, 689–699
15 von Schwedler, U. K., Stuchell, M., Muller, B., Ward, D. M., Chung, H. Y., Morita, E., Wang, H. E., Davis, T., He, G. P., Cimbora, D. M. et al. (2003) The protein network of HIV budding. Cell **114**, 701–713
16 Chen, B., Borinstein, S. C., Gillis, J., Sykes, V. W. and Bogler, O. (2000) The glioma-associated protein SETA interacts with AIP1/Alix and ALG-2 and modulates apoptosis in astrocytes. J. Biol. Chem. **275**, 19275–19281
17 Chatellard-Causse, C., Blot, B., Cristina, N., Torch, S., Missotten, M. and Sadoul, R. (2002) Alix (ALG-2-interacting protein X), a protein involved in apoptosis, binds to endophilins and induces cytoplasmic vacuolization. J. Biol. Chem. **277**, 29108–29115
18 Katoh, K., Shibata, H., Suzuki, H., Nara, A., Ishidoh, K., Kominami, E., Yoshimori, T. and Maki, M. (2003) The ALG-2-interacting protein Alix associates with CHMP4b, a human homologue of yeast Snf7 that is involved in multivesicular body sorting. J. Biol. Chem. **278**, 39104–39113
19 Schmidt, M. H., Hoeller, D., Yu, J., Furnari, F. B., Cavenee, W. K., Dikic, I. and Bogler, O. (2004) Alix/AIP1 antagonizes epidermal growth factor receptor downregulation by the Cbl-SETA/CIN85 complex. Mol. Cell. Biol. **24**, 8981–8993
20 Nebreda, A. R. and Ferby, I. (2000) Regulation of the meiotic cell cycle in oocytes. Curr. Opin. Cell Biol. **12**, 666–675
21 Ferrell, Jr, J. E. (1999) *Xenopus* oocyte maturation: new lessons from a good egg. BioEssays **21**, 833–842
22 Maller, J. L. (1990) MPF and cell cycle control. Adv. Second Messenger Phosphoprotein Res. **24**, 323–328
23 Che, S., Weil, M. M., Nelman-Gonzalez, M., Ashorn, C. L. and Kuang, J. (1997) MPM-2 epitope sequence is not sufficient for recognition and phosphorylation by ME kinase-H. FEBS Lett. **413**, 417–423
24 Belle, R., Cormier, P., Poulhe, R., Morales, J., Huchon, D. and Mulner-Lorillon, O. (1990) Protein phosphorylation during meiotic maturation of *Xenopus* oocytes: cdc2 protein kinase targets. Int. J. Dev. Biol. **34**, 111–115
25 Che, S., El-Hodiri, H. M., Wu, C. F., Nelman-Gonzalez, M., Weil, M. M., Etkin, L. D., Clark, R. B. and Kuang, J. (1999) Identification and cloning of Xp95, a putative signal transduction protein in *Xenopus* oocytes. J. Biol. Chem. **274**, 5522–5531
26 Pan, S., Wang, R., Zhou, X., He, G., Koomen, J., Kobayashi, R., Sun, L., Corvera, J., Gallick, G. E. and Kuang, J. (2006) Involvement of the conserved adaptor protein Alix in actin cytoskeleton assembly. J. Biol. Chem., 10.1074/jbc.M602263200

27 Zeller, M. and Konig, S. (2004) The impact of chromatography and mass spectrometry on the analysis of protein phosphorylation sites. Anal. Bioanal. Chem. **378**, 898–909
28 Liang, Y., Kurakin, A. and Roizman, B. (2005) *Herpes simplex* virus 1 infected cell protein 0 forms a complex with CIN85 and Cbl and mediates the degradation of EGF receptor from cell surfaces. Proc. Natl. Acad. Sci. U.S.A. **102**, 5838–5843
29 Steen, H., Jebanathirajah, J. A., Rush, J., Morrice, N. and Kirschner, M. W. (2006) Phosphorylation analysis by mass spectrometry: myths, facts, and the consequences for qualitative and quantitative measurements. Mol. Cell. Proteomics **5**, 172–181
30 Agromayor, M. and Martin-Serrano, J. (2006) Interaction of AMSH with ESCRT-III and deubiquitination of endosomal cargo. J. Biol. Chem. **281**, 23083–23091
31 Tsang, H. T., Connell, J. W., Brown, S. E., Thompson, A., Reid, E. and Sanderson, C. M. (2006) A systematic analysis of human CHMP protein interactions: additional MIT domain-containing proteins bind to multiple components of the human ESCRT III complex. Genomics **88**, 333–346
32 Nakamura, M., Tanaka, N., Kitamura, N. and Komada, M. (2006) Clathrin anchors deubiquitinating enzymes, AMSH and AMSH-like protein, on early endosomes. Genes Cells **11**, 593–606
33 Segura-Morales, C., Pescia, C., Chatellard-Causse, C., Sadoul, R., Bertrand, E. and Basyuk, E. (2005) Tsg101 and Alix interact with murine leukemia virus Gag and cooperate with Nedd4 ubiquitin ligases during budding. J. Biol. Chem. **280**, 27004–27012
34 Sakaguchi, T., Kato, A., Sugahara, F., Shimazu, Y., Inoue, M., Kiyotani, K., Nagai, Y. and Yoshida, T. (2005) AIP1/Alix is a binding partner of *Sendai* virus C protein and facilitates virus budding. J. Virol. **79**, 8933–8941
35 Harvey, S. L., Charlet, A., Haas, W., Gygi, S. P. and Kellogg, D. R. (2005) Cdk1-dependent regulation of the mitotic inhibitor Wee1. Cell **122**, 407–420
36 Matsuo, H., Chevallier, J., Mayran, N., Le Blanc, I., Ferguson, C., Faure, J., Blanc, N. S., Matile, S., Dubochet, J., Sadoul, R. et al. (2004) Role of LBPA and Alix in multivesicular liposome formation and endosome organization. Science **303**, 531–534
37 Katoh, K., Shibata, H., Hatta, K. and Maki, M. (2004) CHMP4b is a major binding partner of the ALG-2-interacting protein Alix among the three CHMP4 isoforms. Arch. Biochem. Biophys. **421**, 159–165
38 Schmidt, M. H., Chen, B., Randazzo, L. M. and Bogler, O. (2003) SETA/CIN85/Ruk and its binding partner AIP1 associate with diverse cytoskeletal elements, including FAKs, and modulate cell adhesion. J. Cell. Sci. **116**, 2845–2855
39 Kodama, A., Lechler, T. and Fuchs, E. (2004) Coordinating cytoskeletal tracks to polarize cellular movements. J. Cell Biol. **167**, 203–207
40 Schweitzer, J. K., Burke, E. E., Goodson, H. V. and D'Souza-Schorey, C. (2005) Endocytosis resumes during late mitosis and is required for cytokinesis. J. Biol. Chem. **280**, 41628–41635
41 Barr, F. A. (2002) Inheritance of the endoplasmic reticulum and Golgi apparatus. Curr. Opin. Cell Biol. **14**, 496–499

Received 23 August 2006; accepted 18 September 2006
Published as BJ Immediate Publication 18 September 2006, doi:10.1042/BJ20061287